6332

SSD-TDR-63-36

REPORT NO.
TDR-169(3230-11)TN-11

Photoelastic Analyses of Thermal Stresses in Notched Shells and Beams

26 FEBRUARY 1963

Prepared by
C. H. TSAO, A. CHING, and S. OKUBO
Aerodynamics and Propulsion Research Laboratory

Prepared for COMMANDER SPACE SYSTEMS DIVISION
UNITED STATES AIR FORCE
Inglewood, California

LABORATORIES DIVISION • AEROSPACE CORPORATION
CONTRACT NO. AF 04(695)-169

SSD-TDR-63-36

Report No.
TDR-169(3230-11)TN-11

PHOTOELASTIC ANALYSES OF THERMAL STRESSES IN NOTCHED SHELLS AND BEAMS

Prepared by

C. H. Tsao, A. Ching, S. Okubo
Aerodynamics and Propulsion Research Laboratory

AEROSPACE CORPORATION
El Segundo, California

Contract No. AF 04(695)-169

26 February 1963

Prepared for

COMMANDER SPACE SYSTEMS DIVISION
UNITED STATES AIR FORCE
Inglewood, California

ABSTRACT

Progress in the program to determine the optimum notch geometry to minimize the thermal stresses in a notched nose cone or leading edge is discussed.

Theoretical analyses, which have been made on the thermal stresses in shells under nonlinear temperature gradients, show that shells behave like beams.

Photoelasticity was selected as the most accurate and suitable method for investigating notch geometries. The creep properties of Homalite 100, which is used for the photoelastic models, were studied, and the results show that the autocalibration method, applicable only when the amount of creep is proportioned to stress, is true for Homalite 100. The results of an investigation of a number of notched beams by photoelastic methods are presented.

CONTENTS

FIGURES

NOMENCLATURE

a	Semi-major axis of ellipse
b	Semi-minor axis of ellipse
C	A constant
d	Depth of notch
E	Modulus of elasticity
h	Thickness
k	Stress concentration factor
M	Bending moment
p	Applied load
r	Radial distance from center
r_1	Inner radius
r_2	Outer radius
T	Temperature
ΔT	Difference in temperature between the inner and outer surfaces
t	Width
u	Radial displacement
x, y, z	Cartesian coordinates
α	Coefficient of linear thermal expansion
ϵ_θ	Normal strain along the circumferential direction
ϵ_r	Normal strain along the radial direction
ν	Poisson's ratio
σ	Unit stress
σ_θ	Normal stress along the circumferential direction
σ_r	Normal stress along the radial direction
σ_x	Normal stress along the longitudinal direction

I. INTRODUCTION

The objective of this program is to determine the optimum notch geometry to minimize the thermal stresses in a notched nose cone or leading edge.

Theoretical analyses have been made on the thermal stresses in shells under nonlinear temperature gradients. It is shown that even for nonlinear thermal gradients, the shells behave like beams. The analogy between the thermal stresses in shells and in beams is therefore fully established. This theoretical analysis is given in Sect. II.

Presently, a very serious problem exists in the prevention of failures of non-ablative nose cones and leading edges subjected to a high temperature differential between the outer and inner surfaces. The large differences in thermal expansion between the two surfaces produce sufficiently high tensile stresses on the inside surface to produce rupture. One promising method of reducing this high tensile stress is to allow the outer surface to expand with minimum restraint by the introduction of a network of surface notches. The notch spacing and depth will depend upon the temperature differential and the coefficient of thermal expansion of the nose cone or leading edge material. The geometry of the notch bottom will most likely be of an elliptical shape for a minimum stress concentration corresponding to a particular notch depth.

For investigating the various notch geometries to be put on the outside surfaces of nose cones and leading edges to reduce the thermal stresses, photoelasticity was selected as the most accurate and suitable method. In a previous report (Ref. 1), it has been established that for a linear thermal gradient the behavior of shells is quite similar to that of beams so that shells may be simulated by beams in thermal stress investigations. In addition, an equivalence relationship was set up between a linear thermal loading

and a mechanical loading. Notched shells under linear thermal gradient may therefore be simulated by notched beams under an equivalent mechanical loading. In the current reporting period, numerous notched beams have been investigated by photoelastic methods. The results are given in Sect. III.

II. THEORETICAL ANALYSES

Theoretical analyses have been made on the thermal stresses in shells under nonlinear temperature gradients.

A. HOLLOW SPHERE

For a hollow sphere with an arbitrary thermal gradient in direction of thickness (Fig. 1), the governing differential equation can be shown to be

$$\frac{d\sigma_r}{dr} + \frac{2}{r}(\sigma_r - \sigma_\theta) = 0 \qquad (1)$$

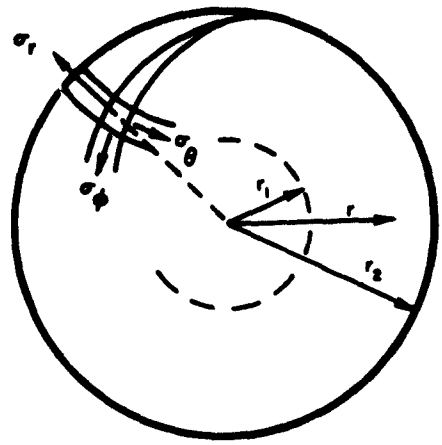

Fig. 1. Hollow Sphere

The stress-strain relations and strain displacement relations are

$$\sigma_r = \frac{E}{(1+\nu)(1-2\nu)}[(1-\nu)\epsilon_r + 2\nu\epsilon_\theta - (1+\nu)\alpha T]$$

$$\sigma_\theta = \frac{E}{(1+\nu)(1-2\nu)}[(\epsilon_\theta + \nu)\epsilon_r - (1+\nu)\alpha T]$$

$$\epsilon_r = \frac{du}{dr}$$

$$\epsilon_\theta = \frac{u}{r}$$

From the boundary conditions, the radial stress is zero on the inner and on the outer surfaces, and the following solution of σ_θ can be obtained for thick hollow spheres

$$\sigma_\theta = \frac{E}{(1-\nu)}\left[\frac{2r^3 + r_1^3}{r^3\left(r_2^3 - r_1^3\right)}\int_{r_1}^{r_2} \alpha T r^2\, dr + \frac{1}{r^3}\int_{r_1}^{r} \alpha T r^2\, dr - \alpha T\right] \tag{2}$$

Introducing a new variable, e, defined by $e = r - r_1$, Eq. (2) becomes

$$\sigma_\theta = \frac{E}{(1-\nu)}\left[\frac{2(r_1+e)^3 + r_1^3}{(r_1+e)^3\left(r_2^3 - r_1^3\right)}\int_0^{r_2-r_1} \alpha T (r_1+e)^2\, de + \frac{1}{(r_1+e)^3}\int_0^{e} \alpha T (r_1+e)^2\, de - \alpha T\right] \tag{3}$$

For thin shells, $e \ll r_1$, and $r_2 - r_1 \ll r_1$. Hence, the above expression for σ_θ can be simplified into

$$\sigma_\theta = \frac{E}{1-\nu}\left(\frac{\int_{r_1}^{r_2} \alpha T\, dr}{r_2 - r_1}\right) - \alpha T \tag{4}$$

Equation (4) gives the circumferential thermal stress in a thin spherical shell under an arbitrary temperature variation in direction of thickness. The material properties E and ν are constants. The coefficient of linear thermal expansion may vary with temperature.

B. LONG CIRCULAR CYLINDRICAL THIN SHELLS

For long circular cylindrical thin shells with thermal gradient in the wall

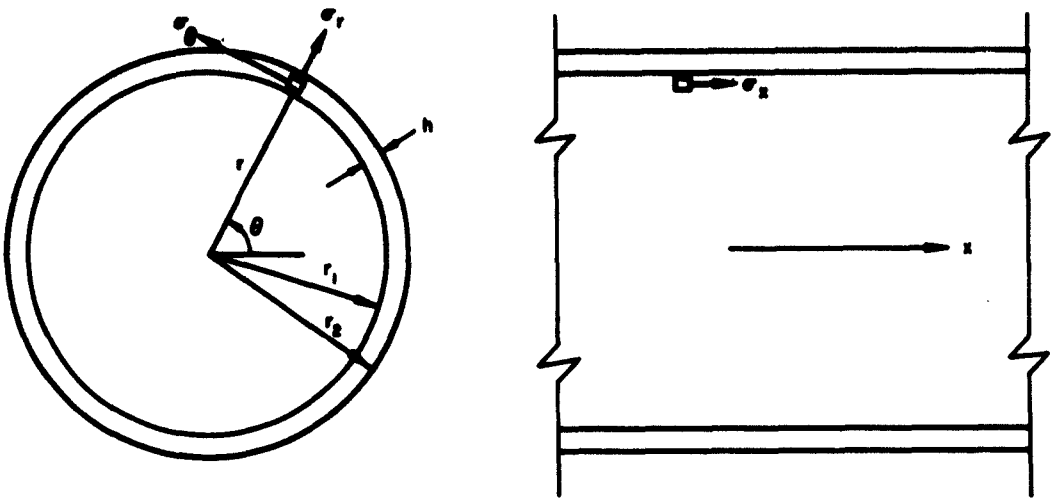

Fig. 2. Long Circular Cylindrical Thin Shells

(Fig. 2), the governing differential equations given in Ref. 2 can be solved to give the thermal stresses in the portions of the shell away from its free ends:

$$\sigma_\theta = \frac{E}{1-\nu}\left(\frac{\int_{r_1}^{r_2} \alpha T \, dr}{r_2 - r_1} - \alpha T\right) \tag{5}$$

Equation (5) gives the circumferential thermal stress in a thin cylindrical shell under an arbitrary temperature variation in direction of thickness. The material properties E and ν are constants. The coefficient of linear thermal expansion may vary with temperature.

C. THIN PLATE

A thin plate in which temperature varies in the y direction only is shown in Fig. 3.

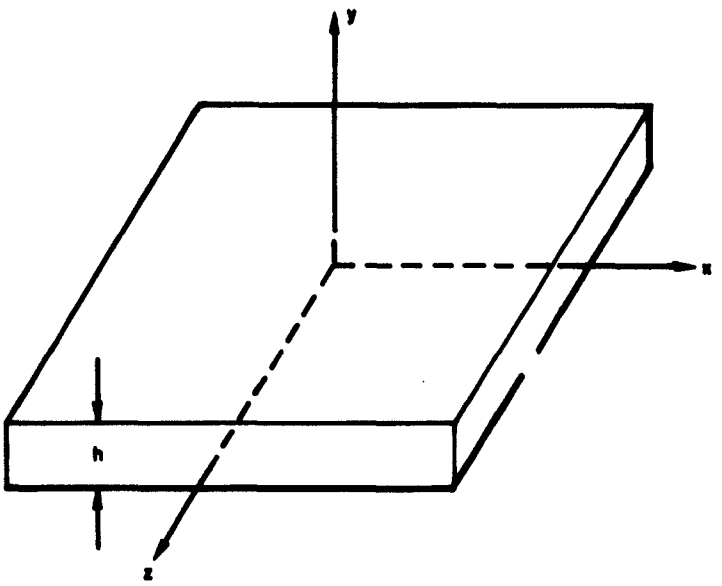

Figure 3. Thin Plate

Following the method outlined in Ref. 3, it can be shown that the thermal stress in a plate restrained against bending only is given by

$$\sigma_x = \frac{-\alpha E T}{1 - \nu} + \frac{1}{h(1 - \nu)} \int_{h/2}^{h/2} \alpha E T \, dy \qquad (6)$$

For constant E and ν, Eq. (6) is simplified into

$$\sigma_x = \frac{E}{1 - \nu}\left(\frac{\int_{-h/2}^{h/2} \alpha T \, dy}{h} - \alpha T\right) \tag{7}$$

D. THIN RECTANGULAR BEAM

A thin rectangular beam in which temperature varies in the y direction only is shown in Fig. 4.

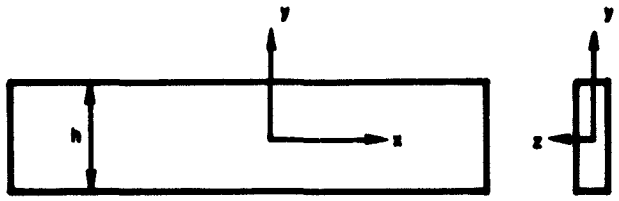

Fig. 4. Thin Rectangular Beam

Following the method outlined in Ref. 3, it can be shown that the thermal stress in a beam restrained against bending only is given by

$$\sigma_x = -\alpha E T + \frac{1}{h}\int_{-h/2}^{h/2} \alpha E T \, dy \tag{8}$$

For constant E and ν, Eq. (8) is simplified into

$$\sigma_x = E\left(\frac{\int_{-h/2}^{h/2} \alpha T \, dy}{h} - \alpha T\right) \tag{9}$$

E. THERMAL STRESS ANALOGY BETWEEN SHELLS AND BEAMS

Equations (4) through (9) show that for any thermal gradient (linear or nonlinear) in direction of thickness, the circumferential thermal stress at any point in the beam is equal to $(1 - \nu)$ times that at the corresponding point in the plate and in the shells. Hence, in the investigation of notches most effective in reducing thermal stresses in shells due to nonlinear as well as linear thermal gradients, experiments may be conducted on beams instead of shells.

III. EXPERIMENTAL ANALYSES

A. TEST PROCEDURE

The material used for the photoelastic models was Homalite 100 which creeps slightly under load. This creep problem was solved by the autocalibration method, which makes the determination of the fringe value of the material unnecessary. Values of stress are given in nondimensional form, as ratios between the fringe order at the selected point and the average fringe order at the sections under pure bending. The creep properties of Homalite 100 were studied, and the results show that the autocalibration method, applicable only when the amount of creep is proportioned to stress, is true for Homalite 100 (see Appendix).

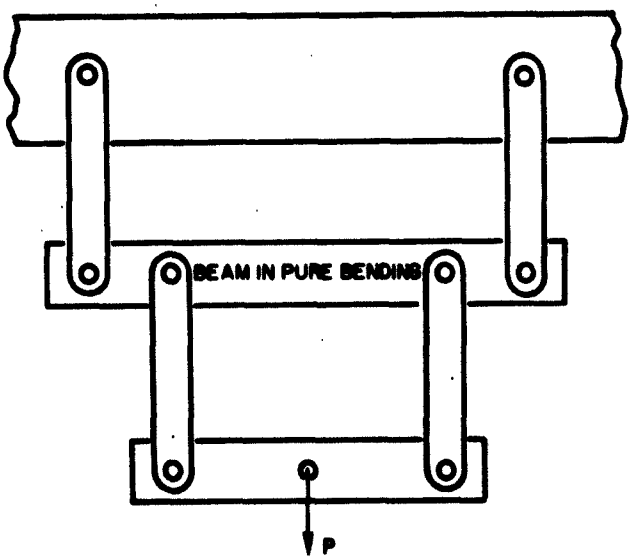

Fig. 5. Loading Arrangement to Obtain Pure Bending

A pure bending moment was used to simulate a linear thermal gradient in the direction of beam thickness. The nominal dimensions of the model beam are 1/4 x 2-1/2 x 16-1/4 in. A schematic of the loading arrangement to obtain pure bending is shown in Fig. 5. This arrangement was used in preference to applying loads on the perimeter of the model by fixed knife edges where friction at the attachment points will introduce secondary bending which has a detrimental influence on the calculated fringe values. Dark field and light field photographs were taken, and points of full- and half-fringe orders were accurately determined from these photographs. Curves were then plotted and extrapolated to the boundaries to obtain the peak or maximum stresses.

B. TEST RESULTS

Tests were conducted on beams with a single notch. The bottom of the notch is of elliptic shape, Fig. 6. Stress concentration factors for a series of beams with varying a/b, d/h, and 2a/h ratios were investigated. The stress concentration factor, k, is defined as

$$k = \sigma_{max}/\sigma_{nom}$$

where σ_{max} is the maximum stress which occurs at the ellipse and was obtained photoelastically, and σ_{nom} is the nominal stress at the bottom of the notch obtained from

$$\sigma_{nom} = \frac{6M}{t(h - d)^2}$$

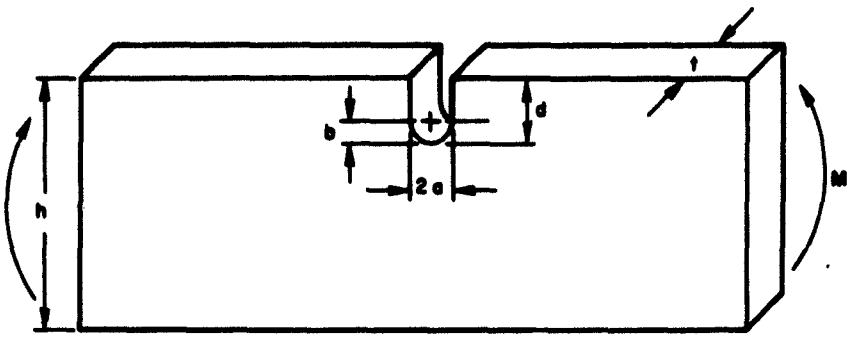

Fig. 6. Beam with a Single Elliptic Notch

In Fig. 7, a plot of the stress concentration factors that were obtained from the tests for d/h ratio of 0.2 is shown. The stress concentration factors for a semicircular notch under the same parameters obtained from Ref. 4 are also shown. It is seen that the lowest stress concentration factor occurs near a/b = 2.5. The isochromatic or stress patterns of Figs. 8-15 show that as a/b increases, the highest stress point shifts from the center of the notch to the two corners. The optimum a/b ratio apparently corresponds to the case where the whole bottom boundary of the notch is uniformly stressed. Tests have shown that the optimum a/b ratio is a function of the d/h ratio.

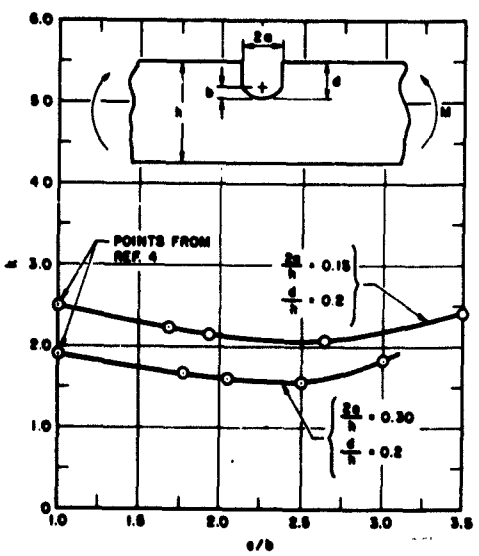

Fig. 7. Stress Concentration Factor, k, for a Single Elliptic Notch in a Flat Bar in Pure Bending

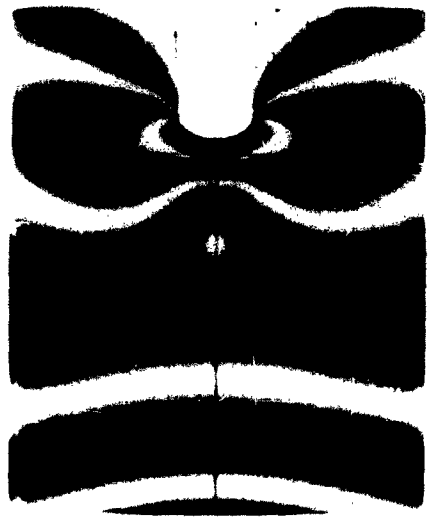

Fig. 8. Isochromatic Pattern of an Elliptical Notched Beam Under Pure Bending; Dark Field, a/b = 1.68, d/h = 0.259, 2a/h = 0.153.

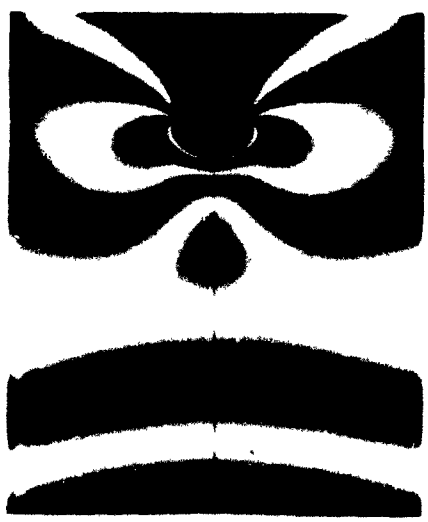

Fig. 9. Isochromatic Pattern of an Elliptical Notched Beam Under Pure Bending; Light Field, a/b = 1.68, d/h = 0.259, 2a/h = 0.153.

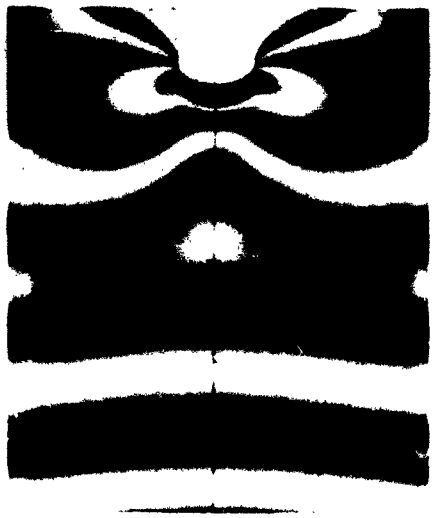

Fig. 10. Isochromatic Pattern of an Elliptical Notched Beam Under Pure Bending; Dark Field, a/b = 1.93, d/h = 0.146, 2a/h = 0.154.

Fig. 11. Isochromatic Pattern of an Elliptical Notched Beam Under Pure Bending; Light Field, a/b = 1.93, d/h = 0.146, 2a/h = 0.154.

Fig. 12. Isochromatic Pattern of an Elliptical Notched Beam Under Pure Bending; Dark Field, a/b = 2.63, d/h = 0.219, 2a/h = 0.154.

Fig. 13. Isochromatic Pattern of an Elliptical Notched Beam Under Pure Bending; Light Field, a/b = 2.63, d/h = 0.219, 2a/h = 0.154.

Fig. 14. Isochromatic Pattern of an Elliptical Notched Beam Under Pure Bending; Dark Field, a/b = 3.5, d/h = 0.218, 2a/h = 0.154.

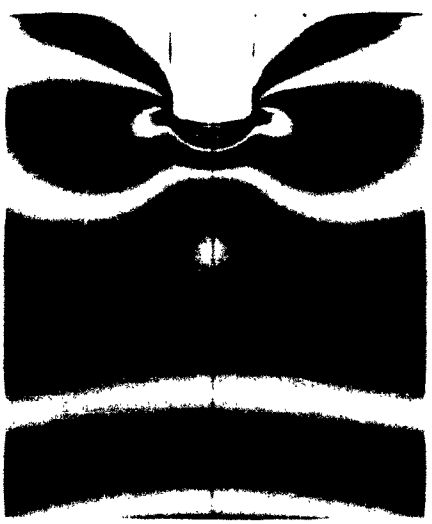

Fig. 15. Isochromatic Pattern of an Elliptical Notched Beam Under Pure Bending; Light Field, a/b = 3.5, d/h = 0.218, 2a/h = 0.154.

IV. TECHNICAL PLANS

During the next reporting period, design curves will be constructed giving the optimum notch shapes for the maximum reduction of thermal stresses. Given the width and depth of a notch, these curves will immediately provide the designers with the best shape and with its corresponding stress concentration factor.

Research will be performed on photothermoelasticity to accurately determine thermal stresses under direct thermal loading and not under a simulated mechanical loading.

APPENDIX

Study of the Creep Properties of Homalite 100

A constant load creep test was conducted for Homalite 100 by applying a concentrated diametral load on a disk (thickness = 0.25 in. and diameter = 2.0 in.) over a period of 24 hr and measuring the fringe order values across the horizontal diameter at various times. The two fringe order curves of Fig. A-1 show that optical creep is directly proportional to stress and

$$\frac{y_a}{y_b} = C$$

is valid for all points on the horizontal diameter.

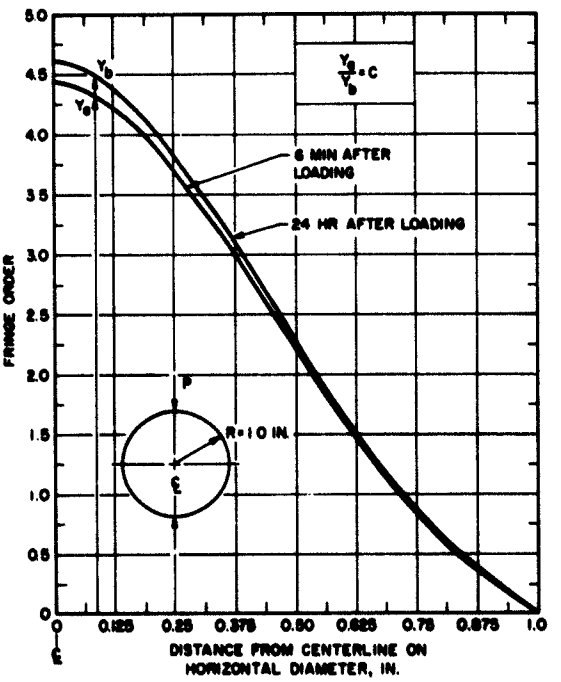

Fig. A-1. Creep Properties of Homalite 100

REFERENCES

1. C. H. Tsao, "Thermal Stresses in Multiple-Notches, Plates, and Shells," ATN-62(9205)-1. Aerospace Corporation, El Segundo, California (6 Sept. 1962).

2. H. S. Tsien and C. M. Cheng, "A Similarity Law for Stressing Rapidly Heated Thin-Walled Cylinders," J. Am. Rocket Soc. 22, 144 (May-June 1952).

3. B. E. Gatewood, Thermal Stresses (McGraw-Hill Book Company Inc., New York, 1957).

4. M. M. Leven and M. M. Frocht, "Stress Concentration Factors for a Single Notch in a Flat Bar in Pure and Central Bending," Proc. of Soc. for Experimental Stress Analysis, C. V. Mahlmann and W. M. Murray, eds. (Soc. of Experimental Stress Analysis, Conn., 1954), Vol. XI, No. 2.

UNCLASSIFIED

Aerospace Corporation, El Segundo, California.
PHOTOELASTIC ANALYSES OF THERMAL STRESSES IN NOTCHED SHELLS AND BEAMS.
Prepared by C. H. Tsao, A. Ching, S. Okubo.
26 February 1963. [29]p. incl. illus.
(Report TDR-169(3230-11)TN-11; SSD-TDR-63-36)
(Contract AF 04(695)-169) Unclassified report

Progress in the program to determine the optimum notch geometry to minimize the thermal stresses in a notched nose cone or leading edge is discussed. Theoretical analyses, which have been made on the thermal stresses in shells under nonlinear temperature gradients, show that shells behave like beams. Photoelasticity was selected as the most accurate and suitable method for investigating notch geometries. The creep properties of Homalite 100, which is used for the photoelastic models, were studied, and the results show that the autocalibration method, applicable only when
(over)

UNCLASSIFIED

UNCLASSIFIED

Aerospace Corporation, El Segundo, California.
PHOTOELASTIC ANALYSES OF THERMAL STRESSES IN NOTCHED SHELLS AND BEAMS.
Prepared by C. H. Tsao, A. Ching, S. Okubo.
26 February 1963. [29]p incl. illus.
(Report TDR-169(3230-11)TN-11; SSD-TDR-63-36)
(Contract AF 04(695)-169) Unclassified report

Progress in the program to determine the optimum notch geometry to minimize the thermal stresses in a notched nose cone or leading edge is discussed. Theoretical analyses, which have been made on the thermal stresses in shells under nonlinear temperature gradients, show that shells behave like beams. Photoelasticity was selected as the most accurate and suitable method for investigating notch geometries. The creep properties of Homalite 100, which is used for the photoelastic models, were studied, and the results show that the autocalibration method, applicable only when
(over)

UNCLASSIFIED

UNCLASSIFIED

Aerospace Corporation, El Segundo, California.
PHOTOELASTIC ANALYSES OF THERMAL STRESSES IN NOTCHED SHELLS AND BEAMS.
Prepared by C. H. Tsao, A. Ching, S. Okubo.
26 February 1963. [29]p. incl. illus.
(Report TDR-169(3230-11)TN-11; SSD-TDR-63-36)
(Contract AF 04(695)-169) Unclassified report

Progress in the program to determine the optimum notch geometry to minimize the thermal stresses in a notched nose cone or leading edge is discussed. Theoretical analyses, which have been made on the thermal stresses in shells under nonlinear temperature gradients, show that shells behave like beams. Photoelasticity was selected as the most accurate and suitable method for investigating notch geometries. The creep properties of Homalite 100, which is used for the photoelastic models, were studied, and the results show that the autocalibration method, applicable only when
(over)

UNCLASSIFIED

UNCLASSIFIED

Aerospace Corporation, El Segundo, California.
PHOTOELASTIC ANALYSES OF THERMAL STRESSES IN NOTCHED SHELLS AND BEAMS.
Prepared by C. H. Tsao, A. Ching, S. Okubo.
26 February 1963. [29]p. incl. illus.
(Report TDR-169(3230-11)TN-11; SSD-TDR-63-36)
(Contract AF 04(695)-169) Unclassified report

Progress in the program to determine the optimum notch geometry to minimize the thermal stresses in a notched nose cone or leading edge is discussed. Theoretical analyses, which have been made on the thermal stresses in shells under nonlinear temperature gradients, show that shells behave like beams. Photoelasticity was selected as the most accurate and suitable method for investigating notch geometries. The creep properties of Homalite 100, which is used for the photoelastic models, were studied, and the results show that the autocalibration method, applicable only when
(over)

UNCLASSIFIED

the amount of creep is proportioned to stress, is true for Homalite 100. The results of an investigation of a number of notched beams by photoelastic methods are presented.

UNCLASSIFIED

UNCLASSIFIED

the amount of creep is proportioned to stress, is true for Homalite 100. The results of an investigation of a number of notched beams by photoelastic methods are presented.

UNCLASSIFIED

UNCLASSIFIED

the amount of creep is proportioned to stress, is true for Homalite 100. The results of an investigation of a number of notched beams by photoelastic methods are presented.

UNCLASSIFIED

UNCLASSIFIED

the amount of creep is proportioned to stress, is true for Homalite 100. The results of an investigation of a number of notched beams by photoelastic methods are presented.

UNCLASSIFIED

UNCLASSIFIED